Journal of Materials Chemistry C

Accepted Manuscript

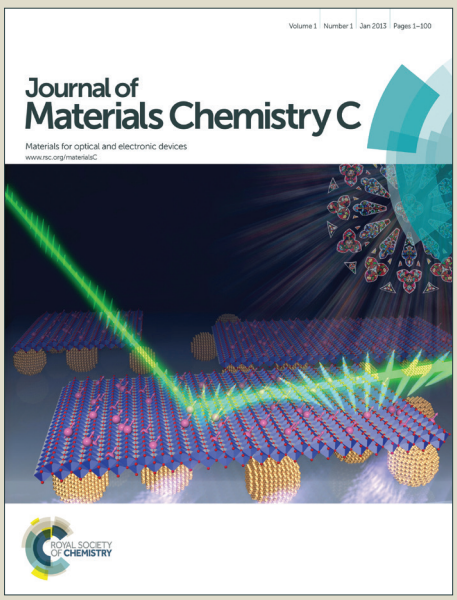

ROYAL SOCIETY OF CHEMISTRY

www.rsc.org/materialsC

Journal of Materials Chemistry C

RSCPublishing

ARTICLE

Maneuvering the Growth of Silver Nanoplate: Use of Halide Ions to Promote Vertical Growth

Cite this: DOI: 10.1039/x0xx00000x

Mun Ho Kim,[*a] Su Kyoung Kwak,[a] Sang Hyuk Im,[b] Jong-Bae Lee,[a] Kil-Yeong Choi,[a] and Doo-Jin Byun[*a]

Received 00th January 2012,
Accepted 00th January 2012

DOI: 10.1039/x0xx00000x

www.rsc.org/

The unique shape and crystalline structure of Ag nanoplates provide an interesting model system for investigating the roles of capping agents in controlling the evolution of the nanostructure shape during growth. This article describes a simple approach to the synthesis of Ag nanoplates with well-controlled shapes in which **halide ions (including Cl^-, Br^-, and I^-)** guides the well-defined kinetically controlled synthetic route. The presence of the iodide ion promoted vertical growth in the nanoplate structure, resulting in small thick nanoplates. The time, during the nanoplate growth process, at which the iodide ion was added, could be adjusted to control the shapes of the Ag nanoplates by controlling the lateral and vertical dimensions of nanoplates. This shape control method permitted tuning of the localized surface plasmon resonance (LSPR) peaks of the Ag nanoplates over the visible and near-IR regions of the spectrum.

Introduction

Metal nanostructures, particularly silver nanostructures, have been extensively studied in recent decades for their potential utility in biological and chemical sensing applications, surface enhanced Raman spectroscopy, and the diagnosis and treatment of disease.[1-3] Most of these applications rely on the unique optical properties of nanostructure, that is, the localized surface plasmon resonance (LSPR). Ag nanostructures typically exhibit LSPR due to the collective oscillations of surface electrons in the presence of incident light. The plasmon band of a nanostructure is modulated by the nanoparticle size, shape, composition, structure (e.g., solid vs. hollow), interparticle distance, and dielectric environment.[4-5] Several strategies have been developed for synthesizing Ag nanostructures with well-defined shapes in an effort to tune the LSPR properties.[6]

Ag nanoplates display fascinating plasmonic properties, including intense quadrupole resonance peaks, and have been in biological and chemical sensing applications.[7] The LSPR of a Ag nanoplate can be tuned by controlling the nanoplate size and aspect ratio. A wealth of chemical methods have been developed to tailor the shapes of Ag nanoplates, such as UV irradiation, thermal treatment, ion etching, and sonochemical treatment, but most of them were based on the post conversion processing methods.[8-9] To the best of our knowledge, direct synthetic methods for producing Ag nanoplates with tunable shapes have not been intensively studied. Successive deposition procedures based on seed-mediated growth have been used to control the Ag nanoplate shape;[10] however, such multistep deposition processes require long process times and significant efforts. A single-step reduction approach would be preferable.

The final shape of a nanocrystal can be defined by the presence of a capping agent that stabilizes certain crystallographic facets. Through its chemical interactions with a metal surface, a capping agent can change the order of the free energies of different crystallographic planes and, thus, their relative growth rates. Preferential capping can drive the addition of Ag atoms to certain crystal facets. The unique shapes and crystalline structures of Ag nanoplates provide an interesting model system for investigating the role of a capping agent in controlling the shape evolution during growth.

Here, we report a new and facile chemical reduction method that yields Ag nanoplates with controllable shapes upon the introduction of **the halide ions (including Cl^-, Br^-, and I^-)** in a well-defined kinetically controlled synthetic route. The present study is different from previous studies that mostly replied on seeded-mediated growth of Ag nanoplates or post transformation process. This single-step procedure is quite simple, and the Ag nanoplates reaction yield (the percentage of plates present among the products) was very high. Interestingly, the time during the nanoplate growth process at which **the halide solution** was added was critical for defining the final shapes. These morphological changes also allow us to finely tune the LSPR peaks of the nanoplates from the visible region to the NIR region. Here, we present a detailed study of the structural, morphological, and spectral changes displayed

during the growth of the Ag nanoplates. These results offer guidelines for controlling Ag nanocrystal shapes in the presence of a capping agent under kinetically controlled conditions.

Experimental Section

Chemicals and Materials.

Silver nitrate ($AgNO_3$, Product No. 209139, 100 g) and PVP (Mw ≈ 29 kDa) were received from Aldrich (USA). Potassium chloride (KCl, Product No. P1597, 500 g), potassium bromide (KBr, Product No. 221864, 25 g), potassium iodide (KI, Product No. 60399, 100 g), and sodium iodide (NaI, Product No. 409286, 1 g) were purchased from Aldrich (USA). N-methyl-2-pyrrolidone (NMP, Product No. 74325, 1 L), used in all reactions, was purchased from Junsei Chemical (Japan). All chemicals were used without further purification. The deionized (DI) water (Product AH365-4, 4 L) used in the reaction was a product of SK Chemicals (Republic of Korea).

Synthesis of Ag Nanoplates.

In a typical synthesis, 1.870 g PVP (Mw ≈ 29 kDa) was dissolved in 8 mL NMP in a 20 mL liquid scintillation vial with a polyethylene liner and a white cap (Research Product International Corp). A 100 μL volume of a 10 mM NMP solution containing halide (KCl, KBr, or KI) was rapidly added to the vial. In the case of KCl, a small amount of DI water was added to the NMP solution containing KCl (the water to NMP w/w ratios was 0.1) because the KCl did not dissolve into pure NMP. Three milliliters of the NMP solution containing $AgNO_3$ (188 mM) was then rapidly added to the vial using a glass pipette. In a typical synthesis, the PVP to $AgNO_3$ weight ratio in the total reaction mixture was fixed at 19.5. After the vial had been capped, the reaction was heated at 100 °C with magnetic stirring for 6 h. The particle growth process was examined at different stages of the reaction by conducting a series of reactions under identical conditions and stopping the reactions at several points over time. The final product was collected by centrifugation and washed with DI water three times to remove most of the NMP and PVP. During the washing process, the suspension was centrifuged at 14,000 rpm for 10 min. Finally, the precipitate was re-dispersed in DI water for further use.

Instrumentation.

TEM and high-resolution TEM imaging technologies were performed using a Phillips Tecnai G220 microscope operated at 300 kV. SEM images were collected using an FEI field-emission microscope (Sirion XL) operated at an accelerating voltage of 10 kV. The TEM (or SEM) sample was prepared by placing a drop of the final product (suspended in DI water) on a carbon-coated copper grid (or silicon wafer), and the sample was dried in a fume hood. The UV-Vis-NIR spectra were recorded at room temperature using a Cary 50 spectrophotometer (Varian, Palo Alto, CA). Photographs were captured using a digital camera (Sony Nex 6).

Results and Discussion

Most previous studies involving chemical reduction methods reported that Ag nanoplates underwent lateral growth along the twin defects and stacking faults to produce larger thin plates.[11-12] Vertical growth that could increase the thickness of the Ag nanoplates was not observed previously in single-step synthesis approaches. These growth mechanisms were related to the Ag nanoplate surface energy. The Ag nanoplate surfaces presented {111} facets at both the top and bottom surfaces, and they contained twin planes with stacking faults on the side facets along the vertical direction. Each nanoplate edge consisted of a {111} facet and a {100} facet, each with a different size.[13] Truncated triangular and hexagonal nanoplates included six edges, half of which featured a {111} facet and half of which featured a {100} facet. The general ordering of the surface energies of the different facets of an fcc metal structure was: $\gamma_{\{111\}} < \gamma_{\{100\}} < \gamma_{\{110\}}$.[14] As the Ag atoms were generated during the reduction reaction, the new Ag atoms were preferentially added to the edges of the nanoplates having surface energies exceeding those of the top and bottom {111} facets. This preferential addition then increased the areas of the top and bottom {111} facets having relatively low surface energies. The primary growth mode was, therefore, lateral, and vertical growth was not extensive.

Terminated with only {111} and {100} facets, the Ag nanoplates provided an interesting model system for investigating the roles of capping agents in the evolution of shape. Since the lateral growth of Ag naonplates was thought to be originated from the high surface energy of {100} facets over {111} facets, the growth behavior could change if the {100} facets are stabilized by capping agents. Others have demonstrated that halide ions, including Cl^-, Br^-, and I^-, bind more strongly to {100} than to {111} facets of Ag crystals, and thereby stabilizing the facets.[15] The addition of halide ions could promote the development of {100} facets; thus, the area ratio of the {100} facets in the final structure could be increased in the presence of halide ions. These additives effect can result in the promotion of vertical growth and thus can be adjusted to tune nanocrystal shape.

We recently reported a method for synthesizing Ag nanoplates in a high yield using chemical reduction approaches.[16] This method involved reducing of $AgNO_3$ by PVP in NMP. During the synthesis, PVP acted as a colloidal stabilizer and a reductant with a weak reducing power, thereby enabling kinetic control over both the nucleation and growth steps. The roles of halide ions in the synthesis of the Ag nanplates were explored by adding small amounts of KCl, KBr, or KI to the reaction mixture. In a typical synthesis, PVP had an average molecular weight of 29 kDa, and its weight ratio relative to $AgNO_3$ was maintained at 19.5. The synthesis was conducted at 100°C in NMP. Fig. 1A shows the Ag nanoplates TEM images of Ag

nanoplates (A) in the absence of halide ions. Fig. 1B-1D show TEM images of the Ag nanoplates after introduction of the halide ions (including Cl^-, Br^-, and I^-). It should be noted that the nanoplate thickness increased remarkably in the presence of halide ions whereas the lateral dimensions decreased. These results indicated that halide ions dramatically affected the synthetic pathways by promoting vertical growth relative to lateral growth via Ag deposition onto nanoplate seed, consistent with our expectations. SEM images of the nanoplates are shown in Fig. S1.

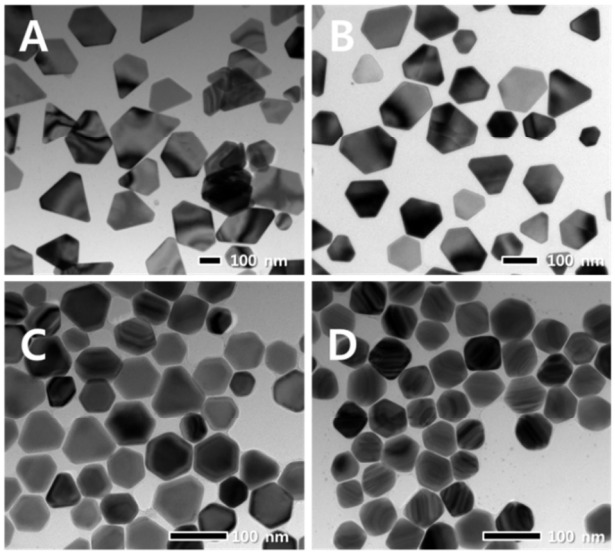

Fig. 1. (A) TEM image of Ag nanoplates formed in the absence of halide ions. TEM images of Ag nanoplates formed in the presence of (B) KCl, (C) KBr, or (C) KI. PVP (29 kDa) to $AgNO_3$ w/w ratio was 19.5. All syntheses were performed at 100 °C over a period of 6 h.

Because halide ions bind strongly to the {100} Ag surfaces, Ag atoms added preferentially to the top and bottom {111} facets, which lengthened {100} facets. The vertical growth in the nanoplate structures was promoted in the order of $Cl^- < Br^- < I^-$, as shown in Fig. 1. The chemisorption of the halide ions on the Ag surfaces increased in an order of $Cl^- < Br^- < I^-$;[17] thus, the iodide ions bound most strongly to {100} facets, to favor the vertical growth of Ag nanoplates. Without the halide ions, the average plate size was 208 nm and the approximate thickness was 28 nm, respectively. The ratio of the lateral dimensions to the vertical dimensions was nearly 7.4. This ratio decreased in the presence of halide ions. As shown in Fig. 1D, the presence of I^- produced some cube-like particles, indicating that the vertical and lateral dimensions of the nanoplates grew to the same degree. These poorly-symmetric particles clearly revealed stacking faults in their inner structures.

The Ag nanoplates growth in the presence of I^- was examined by monitoring the evolution of the shape by conducting a series of reactions under identical conditions and stopping the reactions at several points in time. Fig. 2A-2D show TEM images of Ag nanoplates grown in the absence of I^- and sampled at different reaction times over a 6 h reaction period. At t = 1 h, the sample mainly contained triangular nanoplatets. As the reaction proceeded, the structures evolved to form truncated triangular shapes with sharp edges and corners. During a reaction time of 6h, the nanoplates primarily underwent lateral growth, which increased the lateral dimensions of the nanoplates to yield large thin nanoplates. Fig. 2E-2H revel TEM images of the products obtained after 1, 2, 3, and 6 h reaction times, in the presence of I^-. During the early stages of the reaction, most nanoplates had circular cross-sections. Unlike the particles shown in the Fig. 2A, the particles appeared to be smaller and thicker, as shown in the TEM images. In the presence of I^-, by contrast, the lateral dimension increased preferentially during the first 2 h. Vertical growth was preferred subsequently, and the nanoplate thickness continued to increase up to a reaction time of 6h. And finally, small thick nanoplates were obtained.

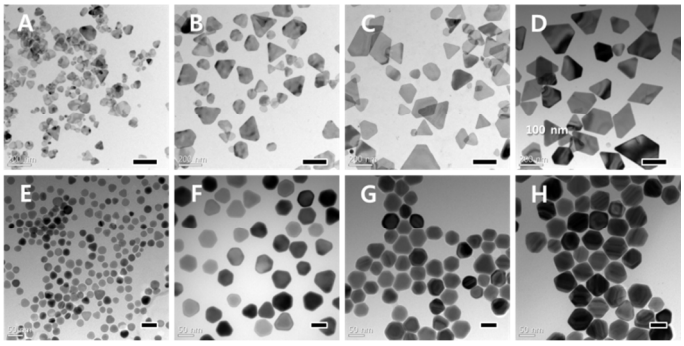

Fig. 2. TEM images of products sampled at different stages of the reaction: (A), (E) t = 1 h, (B), (F) t = 2 h, (C), (G) t = 3 h, and (D), (H) t = 6 h. The synthesis was performed in the absence of I^- (A)-(D) and in the presence of I^- (E)-(H). Scale bar = 200 nm for (A-D) and 50 nm for (E-H).

We further characterized the Ag nanoplates using high-resolution (HR) TEM techniques. Fig. S2 presents a HR TEM image of the nanoplate shown in Fig. 2G. In this image, the (111) stacking faults in the nanoplate are clearly visible, and the vertical dimensions of the particle are analogous to the lateral dimension, indicating that vertical growth was promoted in the presence of I^- ions. The inset of Fig. S2 shows that the lattice spacing of the Ag nanoplates which was 0.23 nm, corresponding to the Ag (111) crystal plane. This measure provided direct evidence for the vertical growth of Ag nanoplates. These results indicated that iodide ions play a pivotal role in the growth of the nanoplates. To confirm that the iodide, and not potassium ions, induced vertical growth in the Ag nanoplates, we replaced the KI with NaI, holding other reaction parameter constant. As shown in Fig. S3, the particle morphology was indistinguishable from that shown in Fig. 1D.

In the present system, the time, during the nanoplate growth process, at which the iodide ions were added could be critical

for preparing a desired shape, and it could be used to effectively control both the size and thickness of as-synthesized Ag nanoplates. Therefore, we monitored the evolution of the shape over the reaction time. Fig. 3A-3E show SEM images of samples obtained after 6 h reaction times, for a given iodide concentration: however, iodide ions were added at the start of the nanoplate growth process (A), or 1 h (B), 2 h (C), 3 h (D), or 4 h (E) into the nanoplate growth process. Fig. 3F shows SEM images of the nanoplates grown in the absence of iodide. In the absence of iodide, the nanoplates primarily underwent lateral growth during the first 6h to form large thin nanoplates. The addition of iodide ions early in the reaction process decreased the lateral dimensions and increased the thickness, as shown in Fig. 3. Interestingly, the lateral dimensions of the nanoplates shown in Fig. 2A-2C and Fig. 3B-3D were similar, confirming that the lateral growth had ceased upon the addition of iodide, and the nanoplates grew vertically. **TEM images of the nanoplates shown in Fig. 3 are shown in Fig. S4, and plots of the average size and thickness of the nanoplates are also shown in Fig. S5.** A schematic diagram illustrating the nanoplates formations in the presence of iodide ions is shown in Fig. 4.

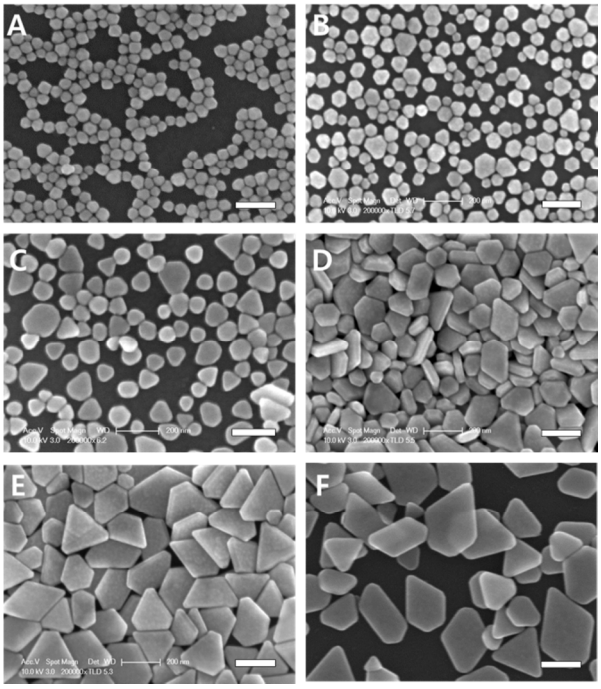

Fig. 3. SEM images of the Ag nanoplate samples obtained from the reaction performed in the presence of a given concentration of I^-; however, I^- solution was added (A) at the start of the reaction, or at (B) t = 1 h, (C) t = 2 h, (D) t = 3h, or (E) t = 4h after the reaction had started. (F) SEM image of the Ag nanoplates formed in the absence of I^-. All syntheses were performed at 100 °C over a period of 6 h. Scale bar = 200 nm for all images.

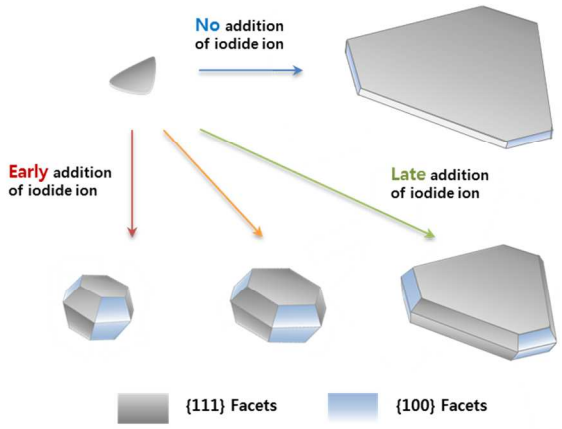

Fig. 4. Schematic diagram illustrating the nanoplates formations in the presence of iodide ions.

Tuning the shape of Ag nanoplates by halides had been studied by other researcher groups. However, the present study should be distinguished from these studies that mostly replied on post transformation process using halide ions as etchants.[9,18] Herein, the iodide ion formed specific binding to the surface of {100} and ultimately promoted vertical growth of Ag nanoplates. When the iodide is insufficiently involved, the vertical growth is not dominant and more anisotropic nanoplates form. When the concentration of I^- decreased to 1/2, the product showed small but thin nanoplate structures as shown in Fig. S6, which confirms that the I^- forms strong capping the edges of plates.

We are not the first group to observe the vertical growth Ag nanoplates in the presence of capping agents. Kitaev et al. reported similar transformation behavior of Ag nanoplates into bi-pyramids and twinned cubes.[19] They attained a mixture of right bipyramids and twinned cubes by heating aqueous dispersions of silver nanoplates with silver nitrate in the presence of PVP and citrate ions. They also reported such structural transformation pathway of Ag nanoplates in the presence of Br^-.[20] These approaches are based on seeded-mediated growth (two-stage modification), and the reaction rate during the transformations was so fast that the control over of nanoparticle size and aspect ratio was not observed. They tried the same experiment in the presence of I^- in the latter, but they found no notable differences. In the present study, the reaction rate based on the reduction of silver ion by PVP went quite slowly and thus the size and aspect ratio of the nanoplates could be controlled as shown in Fig. 3. Furthermore, the difference between Br^- and I^- upon the ability to promote the vertical growth in the nanoplate structure was confirmed.

Iodide ion dramatically affected the synthetic pathways by promoting vertical growth over lateral growth via the

deposition of Ag onto the nanoplate seeds. The size and shape of the resulting nanoplates depended on the time at which the iodide ions were added addition time of iodide ion. The addition time, therefore, could be used to control the resulting LSPR properties, which depend strongly on the size, shape, and thickness of a nanoparticle. **Fig. 5 shows the UV-vis-NIR extinction spectra of the nanoplates shown in Fig. 3. The spectrum of anisotropic Ag nanoplates grown in the absence of iodide ion exhibits several peaks. The peaks at 352 nm and 387 nm can be attributed to the out-of-plane quadrupole and out-of-plane dipole resonances, and the peak shoulder at 500-550 nm corresponds to the in-plane quadrupole resonance.[21-22] The peak at the longest wavelength (at 918 nm) is the contribution of the in-plane dipole resonance.[11]**

In Fig. 5, two distinct features can be found. First, the excitation peaks at the longest wavelengths could be shifted continuously from 918 nm to 444 nm, depending on the addition time of the iodide ion. Specifically, the peak was blue-shifted from 918 nm to 845, 697, 556, 463, or 444 nm in the presence of I^-, due to changes in the shapes of the synthesized Ag nanoplates. The in-plane dipole resonance of the Ag nanoplates became blue-shifted as the edge length decreased. These results confirm that the SPR peaks of the nanoplates could be finely tuned from the visible region to the NIR region by varying the time, during the nanoplate growth process, at which the iodide ions were added. Fig. 5 also shows that the number of peaks in the spectrum decreased as the iodide ion had been added earlier. The early addition of I^- induced nanoplate growth such that the vertical and lateral dimensions were comparable, resulting in the loss of the optical anisotropy identified by the vanishing out-of-plane resonance bands.[20]

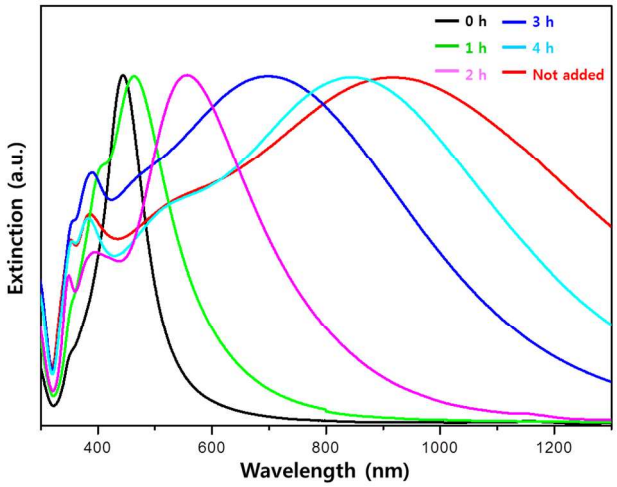

Fig. 5. UV-vis-NIR extinction spectra of the reaction products shown in Fig. 3.

Fig. 6 shows a photograph of eight aqueous dispersions of Ag nanoplates prepared by adding I^- to the reaction mixture at different times during the reaction process. The color could be tuned from yellow to purple to blue. The optical properties resulted from the structural characteristics, which ranged from small thick Ag nanoplates (yielding yellow solutions) to large thin Ag nanoplates (yielding blue solutions).

Fig. 6. Photographs of aqueous dispersions of Ag nanoplates grown in the presence of iodide ions. The times, during the nanoplate growth process, at which the iodide solutions were added to the reaction solution were (from left to right): $t = 0$ h, $t = 1$ h, $t = 1.3$ h, $t = 1.6$ h, $t = 2$ h, $t = 3$ h, or $t = 4$ h after the reaction had begun. The sample farthest to the right was prepared without adding iodide ions.

Conclusions

Ag nanoplates with **tunable** shapes were synthesized in the presence of **halide ions (Cl^-, Br^-, and I^-)** via a well-defined kinetically controlled synthetic route in which the nanoplates grew primarily in the lateral direction over the reaction time. The addition of **halide ions** promoted the development of {100} facets, and thus, vertical growth. **The halides promoted vertical growth in the order of Cl^- < Br^- < I^-.** Small thick nanoplate structures with low degrees of distinct symmetry were obtained in the presence of iodide. The time, during the nanoplate growth process, at which the iodide ions were added could be varied to yield Ag nanoplates with a range of lateral and vertical dimensions. These morphological transformations enabled us to finely tune the LSPR peaks of the Ag nanostructures from the visible to the near-IR region of the spectrum. This work offers a new method for synthesizing Ag nanoplates **with tunable** sizes and shapes in high yields. It also provides important information about how nanoplate shapes may be finely controlled in the presence of a capping agent under conditions of kinetic control.

Acknowledgment

This work was supported in part by the Institutional Research Program (KRICT, KK-1406-B0). This work was partially supported by the Infrastructure Project for Reliability Improvement in Materials and Components Industry, funded by the Ministry of Trade, Industry and Energy (TS133-01R), and the National Research Foundation of Korea (NRF) grants

funded by the Ministry of Science, ICT & Future Planning (MSIP) of Korea under contracts No. NRF-2013R1A2A2A01067999.

Notes and References

[a]Reliability Assessment Center for Chemical Materials, Korea Research Institute of Chemical Technology (KRICT), 141 Gajeong-ro, Yuseong-gu, Daejeon 305-600, Republic of Korea. Fax: +82-42-860-7704; Tel:+82-42-860-7730; E-mail:munho@krict.re.kr, E-mail:djbyun@krict.re.kr

[b]Department of Chemical Engineering, Kyung Hee University, Yongin-si, Kyunggi-do 446-701, Republic of Korea

† Electronic Supplementary Information (ESI) available: [SEM images of Ag nanoplates shown in Fig. 1, HR-TEM images of Ag nanoplates formed in the presence of I^-, TEM image of Ag nanoplates formed in the presence of NaI, and TEM images of Ag nanoplates shown in Fig. 3, TEM image of the nanoplates obtained by the synthesis in which the concentration of iodide decreased to 1/2]. See DOI: 10.1039/b000000x/

1. (a) Y. Xia, Y. Xiong, B. Lim, S. E. Skrabalak, *Angew. Chem. Int. Ed*., 2009, **48**, 60; (b) R. A. Tao, P. Sinsermsuksakul, P. Yang, *Angew. Chem. Int. Ed.*, 2006, **45**, 4597. (c) W. Niu, G. Xu, *Nano Today*, 2011, **6**, 265. (d) A. R. Tao, S. Habas, P. Yang, *Small*, 2008, **4**, 311
2. (a) W. Zhang, J. Yang, X. Lu *ACS Nano* 2012, **6**, 7397 ; (b) X. W. Teng, D. Black, N. J. Watkins, Y. L. Gas, H. Yang *Nano Lett*. 2003, **3**. 261; (c) M. A. El-Sayed *Acc. Chem. Res.*, 2001, **34**, 257; (d) C. J. Murphy, N.R. Jana, *Adv. Mater.*, 2002, **14**, 80; (e) A. R. Rathmell, S. M. Bergin, Y. -L. Hua, Z. -Y. Li, B. J. Wiley *Adv. Mater*., 2010, **22**, 3558.
3. (a) F. Xu, Y Zhu, *Adv. Mater*., 2012, **24**, 5117; (b) L. Hu, S. Kim, J. -Y. Lee, P. Peumans, Y. Cui, *ACS Nano*, 2010, **4**, 2955 ; (c) D. H. Wang, J. K. Kim, G. -H. Lim, K. H. Park, O. O Park, *RSC Adv.*, 2012, **2**, 7268; (d)S. Abalde-Cela, S. Ho, B. Rodrguez-Gonzlez, M. A. Correa-Duarte, R. A. Alvarez-Puebla, L. M. Liz-Marzan, N. A. Kotov *Angew. Chem. Int. Ed.*, 2009, **48**, 5326.
4. (a) S. E. Skrabalak, J. Chen, Y. Sun, X. Lu, L. Au, C. M. Cobley, Y. Xia *Acc. Chem. Res.*, 2008, **41**, 1587. (b) M. H. Kim, J. J. Lee, S. H. Im, D. J. Byun, K. Y. Choi, *CrystEngComm*, 2013, **15**, 6335. (c) B. J. Wiley, S. H. Im, Z. -Y. Li, J. McLellan, A. Siekkinen, Y. J .Xia, *Phys. Chem. B*, 2006, **110**, 15666. (d) M. Rycenga, C. M. Cobley, J. Zeng, W. Li, C. H Moran, Q. Zhang, D.Qin, Y. Xia, *Chem. Rev.*, 2011, **111**, 3669.
5. (a) S. Chen, Y. J. Yang *Am. Chem. Soc.*, 2002, **124**, 5290. (b) M. H. Kim, X. Lu, B. J. Wiley, E. P. Lee, Y. Xia, *J. Phys. Chem. C*, 2008, **112**, 7872; (b) G. Park, C. Lee, D. Seo, H. Song, *Langmuir*, 2012, **28**, 9003; (c) M. Grzelczak, S. A. Mezzasalma, W. Ni, Y. Herasimenka, L. Feruglio, T. Montini, J. Perez-Juste, P. Fornasiero, M. Prato, L. M. Liz-Marzan, *Langmuir*, 2012, **28**, 8826; (d) Y. K. Kim, D. H. Min, *RSC Adv.*, 2014, **4**, 6950.
6. **(a) N. E. Totl, A. F. Smith, C. J. DeSantis, S. E. Skrabalak, *Chem. Soc. Rev.* 2014, *Advance Article* (DOI:10.1039/c3cs60347d); (b) Y. Xia, N. J. Halas, *MRS Bull.*, 2005, 30, 338; (c) Y. Sun. Y. Xia, *J. Am. Chem. Soc.*, 2004, 126, 3892; (d) R. Ringe, M. R. Langille, K. Sohn, J. Zhang, J. Huang, C. A. Mirkin, R. P. Van Duyne, D. M. Marks, *J. Phys. Chem. Lett.* 2012, 3, 1479; (e) M. J. Mulvihill, X. Y. Ling, J. Henzie, P. Yang, *J. Am. Chem. Soc.*, 2010, 132, 268; (f) X. Xia, J. Zeng, B. McDearmon, Y. Zheng, Q. Li, Y. Xia, *Angew. Chem. Int. Ed.*, 2011, 50, 12542; (g) C. Sue, G. S. Metraux, J. E. Millstone, C. A. Mirkin, *J. Am. Chem. Soc.*, 2008, 130, 8337; (h) C. Cobley, M. Rycenga, F. Zhou, Z. Li, Y. Xia, *J. Phys. Chem. C*, 2009, 113, 16975.**
7. (a) C. Gao, Z. Lu, Y. Liu, Q. Zhang, M. Chi, Y. Yin, *Angew. Chem. Int. Ed.*, 2012, **51**, 5629; (b) M. D. Malinsky, K. L. Kelly, G. C. Schatz, R. P. Van Duyne, J. *Am. Chem. Soc.*, 2001, **123**, 1471; (c) H. K. Sung, S. Y. Oh, C. Park, Y. Kim, *Langmuir*, 2013, **29**, 8978; (d) X. L. Guevel, F. Y. Wang, O. Stranik, R. Nooney, V. Gubala,; C. McDonagh, B. D. MacCraith, *J. Phys. Chem. C*, 2009, **113**, 16380.
8. (a) Q. Zhang, J. Ge, T. Pham, J. Goebl, Y. Hu, Z. Lu, Y. Yin, *Angew. Chem. Int. Ed.,* 2009, **48**, 3516; (b) B. Tang, J. An, X. Zheng, X. Xu, D. Li, J. Zhou, B. Zhao, W. Xu, *J. Phys. Chem. C*, 2008, **112**, 18361; (c) B. Tang, S. Xu, X. Hou, J. Li, L. Sun, W. Xu, X. Wang, *ACS Appl. Mater. Interfaces*, 2013, **5**, 646 ; (d) M. Liu, M. Leng, C. Yu, X. Wang, C. Wang, *Nano Res.*, 2010, **3**, 843.
9. (a) J. An, B. Tang, X. Zheng, J. Zhou, F. Dong, S. Xu, Y. Wang, B. Zhao, W. Xu, *J. Phys. Chem. C*, 2008, **112**, 15176; (b) X. Jiang, Q. Zeng, A. Yu, *Langmuir*, 2007, **23**, 2218 ; (d) M. Kim, Y. W. Lee, D. Kim, S. Lee, S. R. Ryoo, D. H. Min, S. B. Lee, S. W. Han, *ACS Appl. Mater. Interfaces*, 2012, **4**, 5038 ; (e) B. Tang, X. Xu, J. An. B. Zhao, W. Xu, J. R. Lombardi, *Phys. Chem. Chem. Phys*, 2009, **11**, 10286.
10. (a) J. Zheng, X Xia, m. Rycenga, P. Henneghan, Q. Li, Y. Xia, *Angew. Chem. Int. Ed.*, 2011, **50**, 244; (b) Q. Zhang, Y. Hu, S. Guo, J. Goebl, Y. Yin, *Nano Lett.*, 2010, **10**, 5037.
11. (a) K. L. Shuford, M. A. Ratner, G. C. Schatz, *J. Chem. Phys.*, 2005, **123**, 114713; (b) J. E. Millstone, G. S. Metraux, C. A. Mirkin *Adv. Funct. Mater.*, 2006, **16**, 1209; (c) R. Jin, Y. Cao, C. A. Mirkin, K. L. Kelly, G. C. Schatz, J. G. Zheng *Science*, 2001, **294**, 1901; (d) Y. Sun, M. Mayers, Y. Xia *Nano Lett.*, 2003, **3**, 675; (e) J. Zhag, M. R. Langille, C. A. Mirkin, *J. Am. Chem. Soc.*, 2010, **132**, 12502; (f) S. Chen, D. L. Carroll *Nano Lett.*, 2002, **2**, 1003;
12. (a) I. Pastoriza-Santos, L. M. Liz-Marzan *Nano Lett.*, 2002, **2**, 903; (b) M. Maillard, S. Giorgio, M. -P. Pileni, *Adv. Mater.*, 2002, **14**, 108; (c) Y. Xiong, A. R. Siekkinen, J. Wang, Y. Yin, M. J. Kim, Y. Zhang, *J. Mater. Chem.*, 2007, **17**, 2600. (d) Q. Zhang, Y. Yang, J. Li, R. Iurilli, S. Xie, D. Qin, *ACS Appl. Mater. Interfaces*, 2013, **5**, 6333. (e) Y. Yang, X. L. Zhong, Q. Zhang, L. G. Blackstad, Z. W. Fu, Z. Y. Li, D. Qin *Small, ASAP.* (DOP:10.1002/smll.201302877) .
13. (a) C. Lofton, W. Sigmund, *Adv. Funct. Mater.*, 2005, **15**, 1197; (b) Y. Xiong, I. Washio, J. Chen, M. Sadilek, Y. Xia,

Angew. Chem. Int. Ed., 2007, **46**, 4917.
14. L. Lu, A. Kobayashi, K. Tawa, Y. Ozaki *Chem. Mater.* 2006, **18**, 4894.
15. (a) S. Gomez-Grana, B. Goris, T. Altantzis, C. Fernandez-Lopez, E. Carbo-Argibay, A. Guerrero-Martinez, N. Almora-Barrios, N. Lopez, I. Pastoriza-Santos, J. Perez-Juste, S. Bals, G. Van Tendeloo, L. M. Liz-Marzan, *J. Phys. Chem. Lett*., 2013, **4**, 2209. (b) B. J. Wiley, Y. Xiong, Z.-Y. Li, Y. Yin, Y. Xia, *Nano Lett.*, 2006, **6**, 765; (c) S. Hong, Y. Choi, S. Park *Chem. Mater.*, 2011, **23**, 5375.
16. M. H. Kim, J. J. Lee, J. B. Lee, K. Y. Choi, *CrystEngComm*, 2013, **15**, 4660.
17. O. M. Magnussen, *Chem. Rev.*, 2002, **102**, 679.
18. (a) M. S. Hsu, Y. W. Cao, H. W. Wang, Y. S. Pan, B. H. Lee, C. L. Huang, ChemPhysChem, 2010, 11, 1742.
19. M. McEachran, V. Kitaev, *Chem. Commun*., 2008, 5737.
20. N. Cathcart, A. J. Frank, V. Kitaev, *Chem. Commun*., 2009, 7170.
21. M. Liu, M. Leng, C. Yu, X. Wang, C. Wang, *Nano Res.*, 2010, 3, 843.
22. X. Liu, L. Li, Y. Yang, Y. Yin, C. Gao, *Nanoscale*, 2014, 6, 4513.

Table of Contents

The addition of iodide ion promoted the vertical growth of nanoplate structures in well-defined kinetically controlled synthetic route, resulting in small thick nanoplates.